

Effects of the Column Approximation on Weak-Beam Calculations

BY ALAN L. LEWIS

Physics Department, Natural Sciences II, University of California, Santa Cruz, California 95064, USA

AND ROBERT E. VILLAGRANA

General Atomic Company, PO Box 91608, San Diego, California 92138, USA

(Received 14 February 1978; accepted 5 October 1978)

Abstract

In electron microscope studies of crystal defects, high-resolution detail is known to exist in the weak beams. The most popular calculational tools for predicting and interpreting this detail are systems of ordinary differential equations based on the column approximation. We argue from analytical and numerical studies of Takagi's equation and certain other equations that the column approximation is unreliable for weak beams in the following specific sense. (i) The main image detail will not be where the column approximation would predict, but shifted to the left or the right by easily determined amounts. This shifting has the consequence that dislocation images, from two or more dislocations, will not be separated in space by the same lateral distance as the dislocations themselves unless the dislocations are all the same distance from the exit surface of the crystal. (ii) There is a very interesting fringe structure, due to the interference of waves within the characteristic triangle, that the column-approximation equations will never exhibit; these fringes, which grow in number with specimen thickness, are predicted to occur most prominently in images of point defects.

1. Introduction

In electron microscopy the use of weak beams to form high-resolution images of lattice defects is becoming increasingly commonplace. The most popular scheme for calculating (and thus understanding) such images involves the numerical solution of certain differential equations based upon the column approximation [see Cockayne (1972) for a review]. Clearly, it is of interest to have a general assessment of the reliability of this approximation in various situations of practical interest, and that is our goal here. Various authors (Jouffrey & Taupin, 1967; Howie & Basinski, 1967; Howie & Sworn, 1970; Rühle & Wilkins, 1975) have investigated the effect of relaxing the column approxi-

mation in specific diffracting situations. The conclusion of these authors is that the effect of the approximation on the transmitted beam and any strongly diffracted beams is generally very small; Howie & Sworn (1970) add to this the general conclusion that the approximation is reliable in the case of inner weak beams (that is, any beams propagating between the transmitted and a strongly diffracted beam). However, in the case of outer weak beams, Humphreys & Drummond (1976) have shown that the approximation is generally unreliable. Here we provide some rules for this situation. These rules are largely geometric in nature, and enable one to assess the error inherent in the column approximation.

These geometric considerations follow from the recent work of Lewis & Villagrana (1975) on a particular function, for Takagi's equation, which represented scattering from a mathematical point defect in an otherwise perfect crystal, and also from numerical work that we report here. All of these various differential equations involve the neglect of any extensive diffuse scattering well away from the diffraction maxima and this should always be kept in mind [see Lewis, Hammond & Villagrana (1975) for a discussion on this]. Indeed, the error involved in the whole differential-equation approach to high-energy electron diffraction, when the wave function is expanded in a modified Fourier series, is difficult to assess and clearly more work on this point would be desirable. We expect, however, that our considerations here are of a sufficiently geometric nature that they take on a validity outside of the particular equations which we consider, but future work will have to establish this. In any event, many of our predictions can be tested in various high-resolution experiments.

Our results are easily summarized. First, we argue that the Green function mentioned above is of special importance in understanding weak-beam images. This is because our numerical work on many-beam situations has shown that the analytical solution for the two-beam Green function in Lewis & Villagrana (1975)

captures the two essential features of scattering from a localized defect. The first feature is that image detail, for a particular beam, propagates primarily at an angle ϕ_g to the normal to the crystal entrance surface. This angle is given by $\tan \phi_g = (K_x + g)/K_z$ for the very simplest situation of a set of systematic reflections $\{\mathbf{g}\}$ in the zero-order Laue zone, where z is the coordinate normal to the crystal entrance surface, x is the coordinate normal to reflecting planes, and \mathbf{K} the electron wave vector. The angle ϕ_g equals the Bragg angle when a particular \mathbf{g} lies on the Ewald sphere. In order to emphasize the connection with the hyperbolic nature of Takagi's equation, we suggest calling the ϕ_g 'characteristic angles'. The column approximation sets all of these characteristic angles to zero; consequently, image information in the column approximation always propagates normal to the entrance surface in the z direction. Consider, as an example, weak-beam scattering from a dislocation (weak beams perceive dislocations as very localized defects); in the column approximation there will be an image peak very near the dislocation core that will always remain near the core no matter how far the core is from the exit surface. Without the column approximation, this peak will be seen to move farther and farther from the dislocation core as the distance from the core to the exit surface increases. This is solely a result of the characteristic angle for the weak beam being non-zero. Some samples of this effect are presented in the text. The second feature captured by the Green function is the interference that develops between beams propagating at different angles ϕ_g . This interference results in fringes that extend, for a particular beam, from the main image detail to either the left or the right depending on the beam. For the outer weak beam in which ϕ_g is negative the fringes extend to the right; for the outer weak beam in which ϕ_g is positive the fringes extend to the left (e.g. see Figs. 2 and 3). In the column approximation these fringes are completely absent.

The plan of this paper is as follows: first, we present the usual geometric argument for the column approximation that proceeds directly from Takagi's equation; then, we extend this argument by considering a formal expansion for the solutions of that equation in powers of $\tan \phi_g$. The lowest-order term is just the column-approximation solution; the first correction term involves x derivatives of the column-approximation solution, which are large in precisely the high-resolution weak-beam situation. Thus, we are able to see directly why the approximation breaks down in the outer weak beams. Then, we summarize the findings of Lewis & Villagrana (1975) concerning the Green function for point scattering in an otherwise perfect crystal and its relevance for the numerical calculations we present. The defects for which we calculate diffraction contrast images are a vacancy in copper and a dissociated dislocation in copper.

2. Geometric considerations

Let us first recapitulate the geometric argument for the column approximation in high-energy electron diffraction. We consider, for simplicity, a two-dimensional specimen with coordinates x and z as defined in the *Introduction*. Further notation will be exactly the same as in Lewis & Villagrana (1975) and will only be minimally redefined here. Now, under certain assumptions involving the localization of intensity in the diffraction pattern (so that the concept of locally diffracting waves takes on meaning), and the neglect of certain second-derivative terms (very small in the high-energy situation), one can obtain from the Schrödinger equation a system of first-order equations first derived by Takagi:

$$\begin{aligned} \hat{\mathcal{L}}\mathbf{D}(x,z) &\equiv (I\partial/\partial z + B\partial/\partial x)\mathbf{D}(x,z) \\ &= iA(x,z)\mathbf{D}(x,z). \end{aligned} \quad (1)$$

In the n -beam situation the matrices, I , B , and A are $n \times n$, and the column vector \mathbf{D} contains the n diffracted wave amplitudes $d_g(x,z)$. Here I is the identity matrix and B is the diagonal matrix with elements given by $B_{gh} = \delta_{gh} \tan \phi_g$. Thus, the directional-derivative operator $\hat{\mathcal{L}}$ is entirely geometrical in nature, and contains no information about the potential of the crystal. Information about the crystal is contained in the matrix A . In this discussion we will only consider elastic scattering, which means that the A matrix is Hermitian. In a perfect crystal the matrix A becomes a constant in space; so that the integration of (1) becomes trivial for plane-wave boundary conditions yielding $\mathbf{D}(z) = \exp(iAz)\mathbf{D}(0)$. We see from this solution that for a perfect crystal the column approximation is rigorous, since this approximation is implemented by setting B to zero in (1). However, in the case of an imperfect crystal the argument for this approximation is as follows.

First, one has to define a length which characterizes the local rate of change of the strain field of a given defect. Then, when this length is always much larger than a geometric length associated with $\hat{\mathcal{L}}$, the column approximation should be valid. Let us be more precise in our argument. From the column-approximation equations one knows that the controlling length (for a set of systematic reflections $n\mathbf{g}$, where n is an integer) is defined by $\mathcal{A}^{-1} = |\partial[\mathbf{g} \cdot \mathbf{R}(x,z)]/\partial z|$, where \mathbf{R} is a vector function describing the atomic displacements. Now, consider a solution to (1), for plane-wave boundary conditions, at a point P on the exit surface of the crystal. Because the differential operator $\hat{\mathcal{L}}$ is hyperbolic, this solution has a region of determinacy. In our discussion this region is a narrow triangle, because for 100 keV electrons the characteristic angles ϕ_g are typically a few degrees with vertex at P . The base of the triangle is formed by a segment of the entrance surface of the crystal. Next, imagine drawing a line across the

triangle, parallel to the base, at an arbitrary depth z within the crystal. For any such depth, there will be a minimum value of the length $A_{\min}(z)$ as x ranges across the line drawn. Suppose the line drawn has length $l(z)$; then the column approximation to the solution at P should be valid if, for every depth z , $l(z) \ll A_{\min}(z)$.

This argument brings out a number of important features of the column approximation which are of practical importance for numerical calculations. Suppose the strain field we are talking about is associated with a dislocation; then, we can always find a column far enough away from the dislocation so that the above inequality is certain to be satisfied. This is important for numerical solutions (e.g. Howie & Basinski, 1967) of Takagi's or other second-order equations of diffraction theory because sometimes the numerical solution needs to be 'stabilized' with the column-approximation solution at large distances from the defect. Another point is that the argument shows that the 'worst' situation, in the case of point defects or dislocations, is when the point P lies directly below the defect core. In this case the triangle of determinacy will enclose the region in which A reaches a minimum; however, note that the argument also implies that if the defect core is close enough to the exit surface of the crystal, the column approximation will still be valid. This is because the length that one should compare with, at a given depth, is always the width of the triangle *at that depth*. This too has important numerical implications; it means that deviations from the column approximation, in the above sense, 'take time to grow' and thus justifies the use of local interpolation procedures in solving these equations.

What the above argument does not demonstrate, however, is why the column approximation is most likely to break down for outer weak beams, yet often remains reasonable for inner weak beams and strong beams. Howie & Sworn (1970) and Humphreys & Drummond (1976) have put forth geometrical explanations of this observation based on considerations of the dispersion surface. We will complement their arguments by showing how it may also be deduced from the differential equation (1). We will do this by constructing a formal expansion in powers of the small matrix B .

As discussed in Lewis & Villagrana (1975), (1) is equivalent, for plane-wave boundary conditions, to the integral equation

$$\mathbf{D}(x, z) = \mathbf{D}_0(z) + \int_0^z \int_{-\infty}^{\infty} \mathcal{A}(x - x'; z - z') \delta A(x', z') \times \mathbf{D}(x', z') dx' dz', \quad (2)$$

where we have written $A = A_0 + \delta A$, A_0 being the constant perfect-crystal matrix, and \mathbf{D}_0 is the perfect-crystal amplitude given by $\mathbf{D}_0 = \exp(iA_0 z) \mathbf{D}_0(0)$. The

basic object of the theory, the Green function \mathcal{A} , is an $n \times n$ singular (in the distribution sense) matrix which has the integral representation

$$\mathcal{A} = \theta(z - z') (2\pi)^{-1} \int_{-\infty}^{\infty} \exp[ik(x - x') - i(kB - A_0)(z - z')] dk, \quad (3)$$

where $\theta(z - z')$ is the unit step function. To see that \mathcal{A} is in general singular, just set $B = 0$ (the column approximation) to obtain $\mathcal{A}_{\text{col.}} = \theta(z - z') \delta(x - x') \exp[iA_0(z - z')]$, where $\delta(x - x')$ is the usual Dirac delta function. Now, we want to expand (3) formally in powers of B ; there is a complication here because the matrices B and A_0 do not commute. However, if we introduce the commutator operator $[A_0, \dots]$, defined by $[A_0, \dots]B = (A_0B - BA_0)$, $[A_0, \dots]^2 B = [A_0, A_0B - BA_0] = A_0^2 B - 2A_0BA_0 + BA_0^2$, etc., then we can expand the integrand to order B by writing

$$\begin{aligned} & \exp[-i(kB - A_0)(z - z')] \\ &= \exp[iA_0(z - z')] \\ & \times \left[1 + \frac{\{\exp[-i(z - z')A_0, \dots] - 1\}}{[A_0, \dots]} \right. \\ & \left. \times Bk + O(B^2) \right], \end{aligned} \quad (4)$$

where the exponential of the commutator operator is defined by its power series and the operator in the denominator just cancels one power from every term of this series. This expansion can be substituted into (3), and the integral over k becomes trivial, just producing a delta function and a derivative of a delta function to this order. Then one substitutes this result for \mathcal{A} into (2), and obtains an integral equation correct through order B .

For simplicity, let us keep only one term of the power series of the commutator operator that appears in (4); then the integral equation becomes

$$\begin{aligned} \mathbf{D}(x, z) &= \mathbf{D}_0(z) + \int_0^z \delta A(x, z') \mathbf{D}(x, z') dz' \\ &+ B(\partial/\partial x) \int_0^z (z - z') A(x, z') \mathbf{D}(x, z') dz'. \end{aligned} \quad (5)$$

If B were zero, (5) would just be the integral-equation version of the column-approximation equations; thus we can look for a correction to this solution by writing $\mathbf{D}(x, z) = \mathbf{D}_{\text{col.}}(x, z) + \delta \mathbf{D}(x, z)$. Consider the specific situation of a very localized defect so that δA is everywhere very small except at one point a distance z_e from the exit surface; then one obtains from (5), neglecting the term $(\delta A)(\delta \mathbf{D})$, $\delta \mathbf{D}(x, z) = z_e B(\partial/\partial x) \mathbf{D}_{\text{col.}}(x, z)$, which is our final result. More generally, for an

arbitrary defect the first correction always involves derivatives of the column-approximation solution. In terms of components, this reads

$$\delta d_g(x, z) = (\text{constant})z_e(\tan \phi_g)(\partial/\partial x)d_g^{\text{col}}(x, z) \quad (6)$$

for an arbitrary point or line defect whose core is a distance z_e from the exit surface. Equation (6) demonstrates why one should be very suspicious of weak-beam calculations in the column approximation. This is because the high-resolution detail in the weak beams means precisely that the x derivative is large, so that the correction δd_g is large. One also sees from (6) that the inner weak beams are somewhat better behaved in this manner because $\tan \phi_g$ is correspondingly smaller, and we reproduce our previous geometric result that the column approximation will always be valid if the defect is close enough to the exit surface (*i.e.* when $z_e \rightarrow 0$).

This expansion in powers of B , due to its formal nature, is not very useful for practical computations. (We can invent situations where it converges to the wrong result.) Usually, one has no recourse but to solve (2), or equivalently (1), numerically. However, due to the considerations in Lewis & Villagrana (1975) of the behaviour of the Green function, Δ , one can understand the nature of the failure of the column approximation in many instances. Let us summarize these considerations and their implications for weak-beam calculations.

In the two-beam case, Δ can be determined analytically and is found to consist of two terms: a singular diagonal matrix of delta functions and a finite matrix of oscillatory functions. The delta functions are singular on the two characteristics that form the sides of the characteristic triangle whose vertex is at the source point (x', z') and whose base lies on the exit surface of the crystal. These delta functions, of which there is one per beam, represent the propagation of the primary image information; in the column approximation one already has such a delta function, $\delta(x - x')$, which restricts the propagation of image information to straight lines in the z direction. Thus, we can anticipate, and we will see this confirmed by numerical examples, that often the effect of removing the column approximation is merely to send the image information along the angles ϕ_g . We should also like to point out that the numerical evidence of this image shifting that is presented in this paper may be taken as support for the conjecture in Lewis & Villagrana (1975) that the many-beam Green function was qualitatively similar to the two-beam Green function in this respect.

In order to determine just how much the calculated image of the defect will be shifted laterally with respect to an image calculated using the column approximation, one merely constructs a triangle of determinancy with source point (x', z') at the defect core and traces straight lines, for the various beam directions, from the source to the exit surface of the crystal (see

Fig. 1). Then if we form an image of the defect, using the g th maxima, it will be centered at the intersection of the g th characteristic with the exit surface. In other words, for a crystal of thickness t the column-approximation image of the defect will always be located near the point $(x', z = t)$, while the image formed with the g th maxima will be located near the point $(x_g, z = t)$, where

$$x_g = x' + z_e \tan \phi_g \quad (7)$$

and x_g is the x coordinate of the intersection of the g th characteristic with the exit surface. Equation (7) tells us that the column-approximation image will be positionally correct only when the defect is very close to the exit surface of the crystal (*i.e.* as $z_e \rightarrow 0$), or when the g th characteristic is parallel to the z axis so that $\phi_g = 0$.

The second implication of this analytical work is the existence of the oscillatory part of the Green function. This part has no correspondence in the column approximation and so represents qualitatively new behavior. There was some doubt in our analytical work as to whether these oscillatory amplitudes would be present in scattering from a real point defect (as opposed to a mathematical point defect); however, as we show in the next section our numerical work confirms the existence of these fringes.

3. Numerical results

3.1. Point defect

All of the numerical work involves a comparison of the solution of the column-approximation equation, Takagi's equation and the second-order equation which one obtains when the term in $(\partial/\partial x)^2$ from the Schrödinger equation is retained. We shall, for brevity, refer to the last two equations as the hyperbolic and parabolic equations. In no instance here did we detect any significant difference between the solutions to the

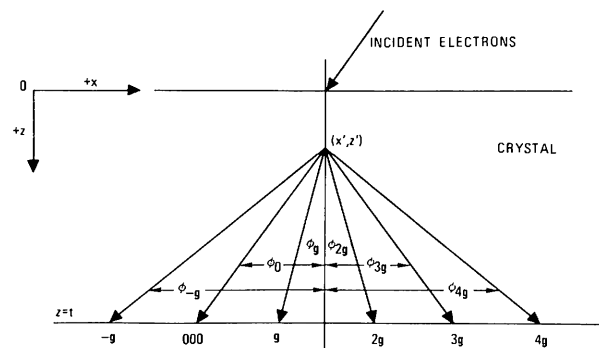


Fig. 1. Sketch of the triangle of determinancy for the six-beam calculations that are presented in this paper; also shown is the coordinate system. The defects considered in this work are centered on the source point (x', z') .

latter equations; this is because although in principle the parabolic equation cannot exhibit a triangle of determinacy, in practice the net effect of the second-derivative term is to contribute a small amount of image spreading outside of the triangle [for a discussion of this point, see Lewis, Hammond & Villagrana (1975)]. Consequently, we will only compare the results obtained with the parabolic equation and the column-approximation equation.

All of the calculations presented in this section involve a set of six systematic reflections $\{ng\}$, with $n = -1, 0, 1, 2, 3, 4$ and scattering parameters appropriate for $g = 202$ in a (111) copper crystal, corrected for absorption and thermal vibration at 300 K. The defects are imaged with 100 keV electrons, and the reflection $3g$ is set at the Bragg condition.

Shown in Figs. 2 and 3 are solutions to the column-approximation and parabolic equations for a vacancy situated at a depth of 400 Å in a crystal 1000 Å thick. We have assumed in these calculations that the strain field of the vacancy can be simulated by that of a cavity in an elastic continuum. In this simplified model the displacement function can be written [for example see Thompson (1969)] as $R(r) = (-r_0^3/r^2)[3\nu/(3\nu + 2\mu r_0)]$, where in these calculations $r_0 = 1$ Å and is the radius of the cavity, $\nu = 0.1$ eV Å⁻² and is the surface energy, and $\mu = 1$ eV Å⁻³ and is the shear modulus.

The solid vertical lines in Figs. 2 and 3 indicate the image shift predicted by (7). In all cases the images

calculated with the column-approximation equation are centered on the x coordinate of the defect, while the geometrically predicted position of the principle image feature of the parabolic-equation calculations lines up nicely with the largest fringe.

Another feature of the parabolic equation is the presence of additional fringes. These fringes are the oscillatory piece of the Green function, Δ , and were explicitly determined from Bessel functions in the two-beam case. Figs. 2 and 3 demonstrate that when a point defect is imaged with the g th maxima these fringes begin at about x_g and decay in a direction opposite to g . In Fig. 2 we also see that as the distance between the vacancy and the exit surface of the crystal increases, so too does the number of fringes. In Lewis & Villagrana (1975) there was a simple rule for the two-beam case: roughly, one fringe is added per extinction distance, as measured from the point defect to the exit surface. However, just as many-beam thickness fringes exhibit a complicated behaviour, one can expect this simple two-beam rule to lose validity in our case here.

There is somewhat of an analogy between these fringes and the phenomenon of Brillouin precursors, first discussed by Brillouin and Sommerfeld in 1914 (see Brillouin, 1960). These precursors occur when a wave pulse propagates (*via* Maxwell's equations) in a dielectric medium: the first thing to arrive on the other side is a very high frequency oscillation which propagates with the speed of light in vacuum and then,

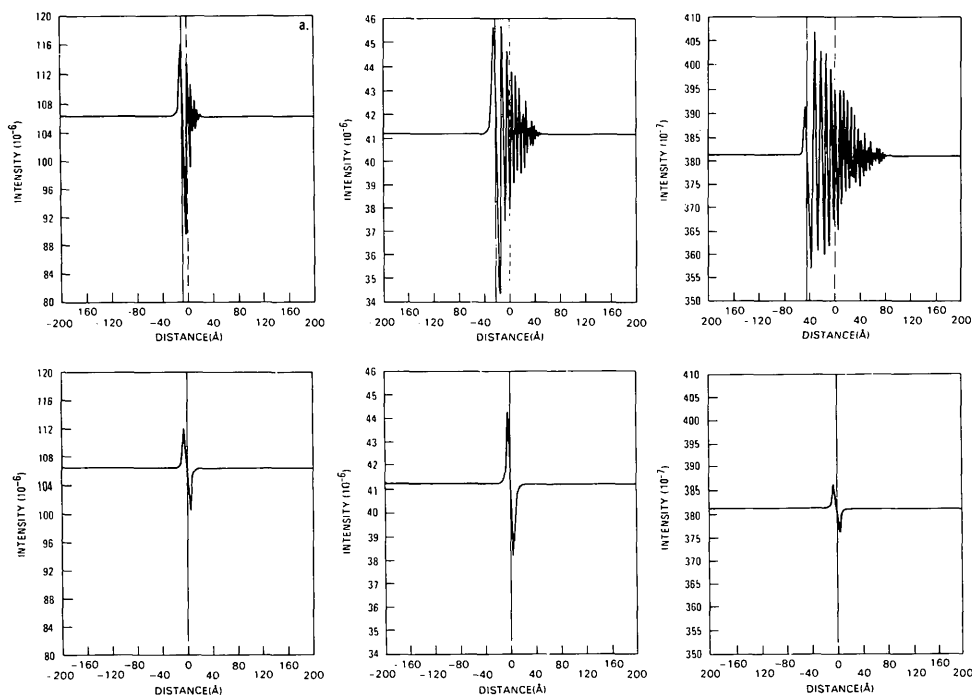


Fig. 2. Computed $-g$ images of a vacancy. In this and the remaining figures the origin of the distance scale has the same x coordinate as the defect; and the solid vertical line indicates the predicted image shift. The equations used for the calculation, specimen thickness, and, when appropriate, the image shift predicted by (7) are: (a) parabolic, 500 Å, -7.2 Å; (b) column approximation, 500 Å; (c) parabolic, 700 Å, -21.7 Å; (d) column approximation, 700 Å; (e) parabolic, 1000 Å, -43.4 Å; and (f) column approximation, 1000 Å.

after the precursors, the original wave packet shows up. In our case, we have somewhat the reverse: the main signal is always 'on the light cone' and showing up 'later' are the rapidly oscillating fringes. The analogy occurs because this behaviour is common to all hyperbolic (wave) operators.

3.2. Line defect

Howie & Sworn (1970) noticed in their calculations that when a weak-beam image of a dislocation was calculated without using the column approximation, it was shifted laterally with respect to the column-approximation calculation. Humphreys & Drummond (1976) add to this observation that the amount of image shifting seems to increase linearly with z_e . In this section we should like to demonstrate that this shifting is also predicted by (7). In order to show this, we will replace the vacancy with a dislocation that lies on a (111) plane and has dissociated according to the reaction: $a/2[\bar{1}01] \rightarrow a/6[\bar{2}11] + a/6[\bar{1}\bar{1}2]$. We will further assume that the lateral separation of the partials is 40 Å, and that all the other crystal and diffraction parameters are the same as those used in the vacancy calculations.

Some results of the dislocation calculations are presented in Figs. 4 and 5. Here we see that (7) predicts the image shift quite well. What is also rather apparent in these figures is that the fringing is associated with the principle image features. For example, in Fig. 4(a) we see that each partial-dislocation peak has fringing rather than the fringing occurring at a single point.

Another striking feature of these calculations, aside from the image shifting and fringing, is the correspondence that exists between the images calculated both with and without the column approximation. Generally, this will not be the case; one can easily design situations involving dislocations at different depths where this correspondence would not hold because of image overlap. Finally, there is an interesting image behaviour

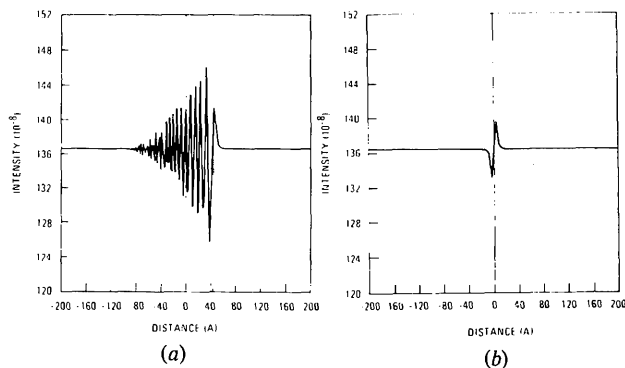


Fig. 3. Computed 4g images of a vacancy in a crystal 1000 Å thick. In (a) the parabolic equation was used, and the amount of image shift predicted by (7) is 43.4 Å. The column-approximation equation was used to calculate (b).

seen in the $-g$ reflection that is independent of the column approximation. Note in Fig. 4(a) and (b) that the peaks corresponding to both partials are in phase, while in Fig. 4(c) and (d) they are out of phase. Now since both partial dislocations are at the same depth, their respective peaks should oscillate in phase if the scattering is maximized at the respective dislocation cores. The fact that they are not in phase indicates that the scattering is maximized at slightly different positions in the respective strain fields of the partial dislocations.

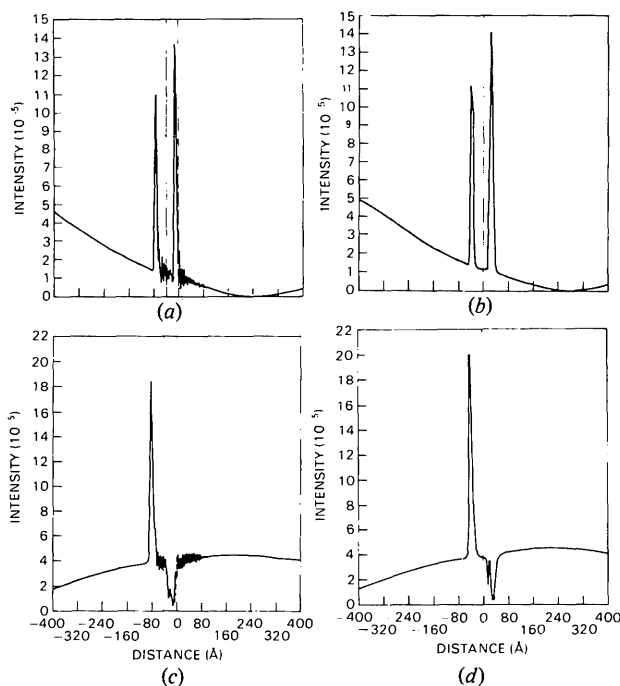


Fig. 4. Computed $-g$ images of a dissociated dislocation. The equations used for the calculation, specimen thickness, and, when appropriate, the image shift predicted by (7) are: (a) parabolic, 900 Å, -36.2 Å; (b) column approximation, 900 Å; (c) parabolic, 1000 Å, -43.4 Å; (d) column approximation, 1000 Å.

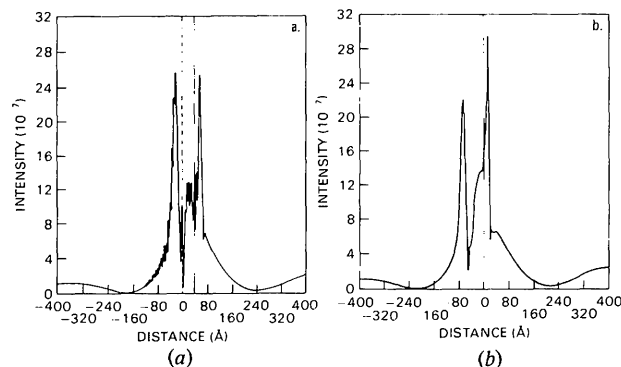


Fig. 5. Computed 4g images of a dissociated dislocation in a crystal 1000 Å thick. In (a) the parabolic equation was used, and the amount of image shift predicted by (7) is 43.4 Å. The column-approximation equation was used to calculate (b).

4. Concluding remarks

It is safe to say that the preponderance of our present knowledge about the electron-microscope contrast behavior of defects in crystals was obtained using diffraction equations based upon the column approximation. However, the use of these equations to describe defect contrast under high-resolution conditions is dangerous. In this paper we have demonstrated two ways (image shifting and fringing) in which the column-approximation equations fail to predict contrast for point and line defects. However, we have not discussed the visibility of the fringing. Our feeling is that if it can be resolved, it will most probably be visible in weak-beam images of point defects and very small precipitates. Of course, this question will only be answered by the experimentalist. In a future paper we will discuss the effect of the column approximation on the calculation of images of planar defects.

The authors would like to thank Dr A. Lannes for helpful discussions, and Mr D. R. Wall and Ms B. J.

Jones for assistance in the final preparation of this manuscript.

References

- BRILLOUIN, L. (1960). *Wave Propagation and Group Velocity*. New York: Academic Press.
- COCKAYNE, D. J. H. (1972). *Z. Naturforsch. Teil A*, **27**, 452–460.
- HOWIE, A. & BASINSKI, Z. A. (1967). *Philos. Mag.* **17**, 1039–1063.
- HOWIE, A. & SWORN, C. H. (1970). *Philos. Mag.* **22**, 861–864.
- HUMPHREYS, C. J. & DRUMMOND, R. A. (1976). *Proceedings of the 6th European Regional Congress on Electron Microscopy*, Jerusalem, Vol. 1, pp. 142–146.
- JOUFFREY, B. & TAUPIN, D. (1967). *Philos. Mag.* **16**, 703–715.
- LEWIS, A. L., HAMMOND, R. B. & VILLAGRANA, R. E. (1975). *Acta Cryst.* **A31**, 221–227.
- LEWIS, A. L. & VILLAGRANA, R. E. (1975). *Acta Cryst.* **A31**, 722–727.
- RÜHLE, M. & WILKINS, M. (1975). *J. Appl. Cryst.* **8**, 222–223.
- THOMPSON, M. W. (1969). *Defects and Radiation Damage in Metals*, pp. 13–17. Cambridge Univ. Press.

Acta Cryst. (1979). **A35**, 282–286

Symmetry- and Composition-Dependent Cumulative Distributions of the Normalized Structure Amplitude for Use in Intensity Statistics

BY URI SHMUELI

Department of Chemistry, Tel-Aviv University, 61390 Ramat Aviv, Tel-Aviv, Israel

(Received 21 July 1978; accepted 25 August 1978)

Abstract

Centric and acentric cumulative distribution functions of the normalized structure amplitude, which explicitly account for the presence of outstandingly heavy atoms in crystals of any symmetry, have been derived. These cumulative distributions can now be readily evaluated for all triclinic, monoclinic and orthorhombic space groups, with the exceptions of *Fdd2* and *Fddd*, and thus constitute an extension of the commonly employed cumulative distributions based on the Wilson statistics. Expected discrepancies between the distributions derived in this work and the corresponding Wilson-type distributions are illustrated, and their symmetry and composition dependence is discussed in view of relevant applications to intensity statistics.

0567-7394/79/020282-05\$01.00

Introduction

The known methods of intensity statistics, which are applicable to the resolution of space-group ambiguities, can be classified into (A) computation of an experimental average of a function of the structure amplitude and comparison of this average with its theoretical expectation values for the possible space groups, and (B) comparison of experimental and theoretical distributions of the normalized intensity or structure amplitude. Most existing methods of both classes are based on the Wilson (1949) statistics, according to which the structure amplitude from an equal-atom structure, with a large number of atoms in the unit cell, is normally distributed, the distribution parameters being different for the centrosymmetric and noncentro-

© 1979 International Union of Crystallography